

Study on re-adhesion control by monitoring excessive angular momentum in electric railway tractions

Takafumi Hara and Takafumi Koseki

Department of Electrical Engineering and Information Systems
Graduate School of Engineering, The University of Tokyo
7-3-1 Hongo, Bunkyo-Ku, Tokyo, Japan
Telephone: (+81)3-5841-6791
Email: t_hara@koseki.t.u-tokyo.ac.jp, takafumikoseki@ieee.org

Abstract—Suppression of slip and reduction of friction between rail and wheel are important in railway systems. This paper proposes a novel slip re-adhesion control based on the excessive torque and excessive angular momentum for 4 axle and 2 truck model (1C2M, 1 inverter 2 motor drive system). Effectiveness of the proposed method has been confirmed by mathematical analysis. Furthermore, the proposed method was evaluated by two performance indicators, frictional force reduction and effective utilization of adhesive force. As a result, adhesion characteristic of the proposal method was 7.04 % better than the conventional method. In addition, loss friction force around driving wheel remained unchanged.

I. INTRODUCTION

Electric railway traction has small tractive force which needs to accelerate, so a slip often generates under bad track condition[1] such as fallen leaves and snowfall. It is important to avoid the slip and to use the adhesion phenomenon effectively for acceleration and deceleration in electric railway traction.

Many studies focus on slip re-adhesion control[2]. Slip re-adhesion control that estimates and uses adhesive torque with the disturbance observer has been proposed[3][4]. It has been used in real trains[5]. However, it is not clear whether electric railway traction can re-adhere under bad track condition[1] such as fallen leaves and snowfall.

This paper proposes a new slip re-adhesion control based on excessive torque and excessive angular momentum of 1 axle and 1 body model. In addition, we extent this model for 4 axle and 2 truck model (1C2M, 1 inverter 2 motor drive system). The effectiveness of the proposed method has been confirmed by mathematical analysis. Furthermore, the proposed method was evaluated by two performance indicators, frictional force reduction and effective utilization of adhesive force. In addition, we compared the proposed re-adhesion control with the conventional re-adhesion control [6] and showed the advantages of the proposed re-adhesion control.

TABLE I
PARAMETERS EXPLANATION

Item	Value	Comment
J_R	Inertia moment around wheel	$\text{kg} \cdot \text{m}^2$
J	Equivalent inertia moment of drive axle	$\text{kg} \cdot \text{m}^2$
ω_w	Driving wheel angular velocity	rad/s
G_r	Gear ratio	-
M_R	Equivalent inertia weight around wheel	kg
M	Mass per axle	kg
v_b	Velocity	rad/s
v_s	Slip velocity	m/s
ω_s	Slip angular velocity	m/s
T_m	Motor torque	N-m
T_L	Adhesive torque	N-m
r	Radius of wheel	m
F_d	Travel resistance	N

II. PROPOSED RE-ADHESION CONTROL

A. Excessive torque and excessive angular momentum[7]

In this section, we develop the excessive torque and excessive angular momentum from two equations of motion. Two equations of motion simplified a body and a wheel is shown from Eq. (1) to Eq. (2).

$$J_R \dot{\omega}_w = G_r T_m - T_L \quad (1)$$

$$M \dot{v}_b = \frac{T_L}{r} - F_d \quad (2)$$

$$v_s = r\omega_w - v_b, \omega_s = \omega_w - \frac{v_b}{r} \quad (3)$$

Parameters in this above equations are defined in Table I. We propose to modify rotational equations of the motion as follows. Given that a body is a square and a wheel is a disk, we calculate moments of inertia ($J_R = \frac{1}{4}M_R r^2$, $J = M r^2$). Relation slip between body velocity and wheel speed is described in Eq. (3). Therefore, derivative value of slip angular velocity ($\dot{\omega}_s$) is shown in Eq. (4).

$$\dot{\omega}_s = \frac{1}{J_R} \left\{ G_r T_m - \left(1 + \frac{J_R}{J} \right) T_L + \frac{J_R}{J} r F_d \right\} \quad (4)$$

Slip velocity depends on motor torque, adhesive torque and disturbance torque. Increasing slip velocity will worsen slip.

The excessive torque is defined in Eq. (5).

$$\begin{aligned} T_{ex} &= J_R \dot{\omega}_s \\ &= G_r T_m - \left(1 + \frac{J_R}{J}\right) T_L + \frac{J_R}{J} r F_d \end{aligned} \quad (5)$$

Excessive torque is the difference between motor torque ($G_r T_m$) and adhesive torque ($(1 + \frac{J_R}{J}) T_L$). This torque is the torque that does not contribute to rotate the wheels.

In addition, integral of the excessive torque is given in Eq. (6). We can define integral of the excessive torque as the excessive angular momentum.

$$L_{ex} = \int \left\{ G_r T_m - \left(1 + \frac{J_R}{J}\right) T_L + \frac{J_R}{J} r F_d \right\} dt \quad (6)$$

By using excessive torque and excessive angular momentum, slip angular velocity is given in Eq. (7). Derivative value of slip velocity is given in Eq. (8).

$$\Delta \omega_s = \frac{1}{J_R} \int T_{ex} dt \quad (7)$$

$$\dot{\omega}_s = \frac{1}{J_R} L_{ex} \quad (8)$$

Consequently, slip angular velocity is proportioned to excessive torque. Derivative of slip velocity is proportional to excessive angular momentum. Excessive angular momentum should be as low as possible to stop slip. We can imply that we can estimate slip prevention and slip extent by watching the excessive angular momentum. This vision is shown in Fig. 1.

B. Estimation of adhesive torque

When we calculate the excessive torque (T_{ex}) and the excessive angular momentum (L_{ex}), we need to estimate the adhesive torque as the load torque for an axle.

The disturbance observer to estimate the adhesive torque as the load torque for an axle is given in Eq. (9). This disturbance observer is a homogeneous dimension observer. The estimation of the adhesive torque uses the angular velocity, motor torque and assumption of zero-order dynamics ($\hat{T}_L = 0$). H is the observer gain.

$$\frac{d}{dt} \begin{bmatrix} \hat{\omega}_w \\ \hat{T}_L \end{bmatrix} = \begin{bmatrix} 0 & -\frac{1}{J} \\ 0 & 0 \end{bmatrix} \begin{bmatrix} \hat{\omega}_w \\ \hat{T}_L \end{bmatrix} + \begin{bmatrix} \frac{G_r}{J_R} \\ 0 \end{bmatrix} T_m + H (\hat{\omega}_w - \omega_w) \quad (9)$$

$$y = \begin{bmatrix} 1 & 0 \end{bmatrix} \begin{bmatrix} \hat{\omega}_w \\ \hat{T}_L \end{bmatrix} \quad (10)$$

Slip detection use excessive torque, difference between motor torque ($G_r T_m$) and adhesive torque ($(1 + \frac{J_R}{J}) T_L$). If excessive torque exceeds threshold $T_{ex-threshold}$, the proposed re-adhesion control starts. However, this control re-checks time after τ_1 s (50 mill-sec) from slip detection.

C. Torque command pattern for the re-adhesion

The parameters for different slip time are shown in Table II. Motor torque ($G_r T_m$) and adhesive torque ($(1 + \frac{J_R}{J}) \hat{T}_L - \frac{J_R}{J} r F_d$) of the disturbance is shown in Fig. 2. In this case, we can not estimate disturbance torque, so the excessive angular momentum can not be determined. Consequently, the re-slip

TABLE II
DEFINITION OF THE SLIP TIME

Slip start time	t_{slip}
Slip detection time	t_{detect}
Motor torque down time	t_{Tdown}
Motor torque up time	t_{Tup}
Time from slip detection time to motor torque down time	τ_1
Time from motor torque down time to re-adhesion detection	τ_2

will occur. Given that the disturbance torque of the gradient and the train resistance is constant when train slips, We propose that re-adhesion control can consider the disturbance torque. We propose to deal with re-adhesion control in two road surface conditions.

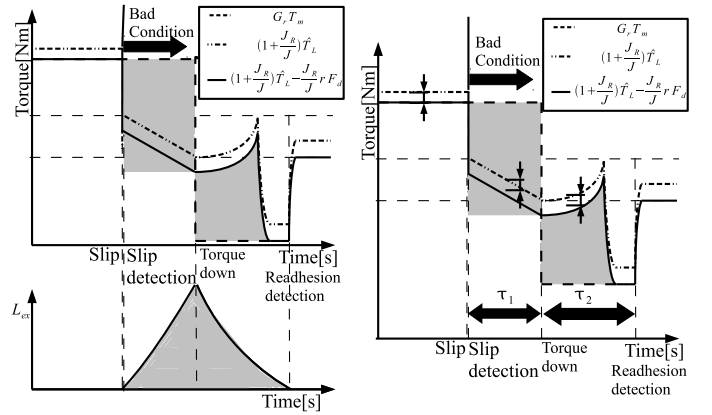


Fig. 1. Excess torque (T_{ex}) and angular momentum (L_{ex})

Fig. 2. Disturbance torque estimation

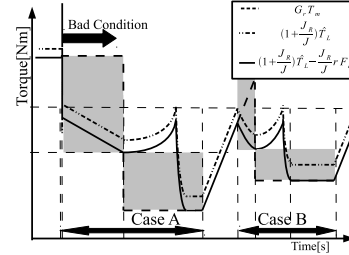


Fig. 3. Case analysis of the proposed re-adhesion control (Case A...Only first, Case B...Second, third,)

- 1) Situation on road surface to change from good condition to bad condition (Case A, only first)
- 2) Situation on road surface to continue bad condition (Case B)

The area shape of the excessive angular momentum changes when torque is constant and linearly increasing. The area shape change of the excessive angular momentum is shown in Fig. 3. When the condition on the road surface is getting worse, we suggest that the excessive angular momentum can approximate a rectangle (Case A). In contrast, when the road surface continues in bad condition, we suggest that excessive angular

momentum can approximate a triangle (Case B). Thus, we can approximately calculate the excessive angular momentum. The excessive angular momentum approximately calculated from rectangle and triangle stays in the safe side, so the real excessive angular momentum will not be larger than the calculated excessive angular momentum.

We suggest that excessive angular momentum after re-adhesion control reduces motor torque can approximate rectangle.

D. Expansion of the proposed re-adhesion control for 4 axle and 2 truck model

It is easy to expand 1C1M (1 inverter 1 motor drive system, Fig. 4 (c)). Because, this proposed re-adhesion control is based on one axle and one body. This proposed re-adhesion control for 1C4M (1 inverter 4 motor drive system, Fig. 4 (a)) is very difficult because of poor information of motor torque and angular velocity of each axle. Thus, we extend 1C2M (1 inverter 2 motor drive system, Fig. 4 (b)) and understand difficulty of parallel induction motor drive system. We consider the following information to expand the proposed re-adhesion control to 4 axle model.

- 1) Average motor torque (Average current value)
- 2) Average angular velocity $\frac{\omega_1 + \omega_2}{2}$ (Average of 1 axle angular velocity ω_1 and 2 axle angular velocity ω_2 , speed sensor-less vector control)
- 3) Average adhesive torque with average motor torque and average angular velocity

It is important to make motor torque smaller than adhesive torque in each axle. In addition, we consider excessive angular momentum preservation based on bad condition axle.

If only 1 axle slips, controller can watch excessive torque, the difference between motor torque and adhesive torque. However, this excessive torque is one-half of 1 axle excessive torque. Therefore, torque down constant k in 4 axle model is about as large as the constant in one axle model. Expansion of the proposed re-adhesion control for 4 axle model is shown in Fig. 5.

1) *Excessive angular momentum from slip detection to torque down:* Excessive angular momentum from slip detection to torque down can approximate rectangle. In addition, it is assumed that it is rare that all of two or more axes cause this the idling at the same time. Therefore, excessive angular momentum of 1 axle is twice as large as excessive angular momentum which a re-adhesion controller watches average of motor and adhesive torque. This idea is shown in Fig. 5. As a result, excessive angular momentum from slip detection to torque down L_{ex, τ_1} is given in Eq. (11).

$$L_{ex, \tau_1} = 2\tau_1 T_{ex} \quad (11)$$

2) *Excessive angular momentum from torque down to torque up:* Excessive angular momentum from torque down to torque up L_{ex, τ_2} is given in Eq. (12). This equation is excessive angular momentum of slipping axle.

$$L_{ex, \tau_2} = \tau_2(k-1)T_{ex}(k > 1) \quad (12)$$

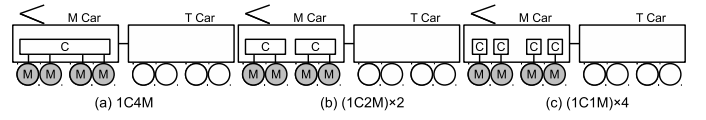


Fig. 4. Drive system of electric railway

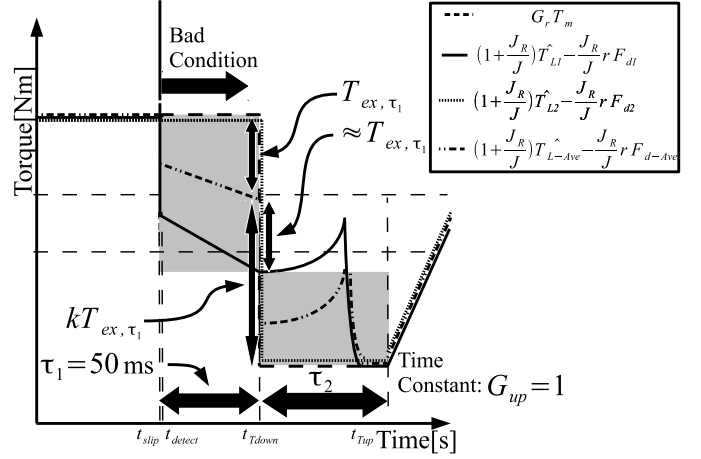


Fig. 5. Expansion of the proposed re-adhesion control for 4 axle model

3) *Time τ_2 derived from preservation of excessive angular momentum:* Time τ_2 derived from preservation of excessive angular momentum (Eq. (11), (12)) is given in Eq. (14).

$$2\tau_1 T_{ex} = \tau_2(k-1)T_{ex}(k > 1) \quad (13)$$

$$\tau_2 = \frac{2}{k-1} \tau_1 \quad (14)$$

Time τ_2 is longer compared with 1C1M (1 inverter 1 motor drive system) because of truck oscillation and axle-weight transfer.

E. Basic torque command pattern

The motor torque command for the re-adhesion is given in Eq. (15) in terms of the motor torque T_m before the slip, the adhesive torque $T_{L-detect}$ when the slip detects and the adhesive torque T_{m-down} when the motor torque reduces. When the motor torque raises, the time constant of the motor torque is G_{up} . This is due to the re-slip if the torque raises in the step-like pattern.

$$T_m^* = \begin{cases} T_m & (t_{slip} < t < t_{Tdown}) \\ T_{m-down} & (t_{Tdown} \leq t \leq t_{Tup}) \\ T_{m-down} + G_{up}(T_m - T_{m-down})(t - t_{Tup}) & (t_{Tup} < t) \end{cases} \quad (15)$$

Reduction of motor torque from slip generation (t_{slip}) to slip detection (t_{detect}) is decided to regulate for the excessive angular momentum as described in Sections II-C and II-D. The motor torque reduction in $t_{slip} < t < t_{detect}$ is shown in Eq. (16).

$$L_{ex, \tau_1} = \tau_2(T_{L-detect} - T_{m-down}) \quad (16)$$

The basic torque command pattern is shown in Table III.

TABLE III
TORQUE PATTERN

Time	Explanation
t_{slip}	Slip generation
↓	Infinitesimal time $T_m^* = T_m$
t_{detect}	Slip detection
↓	$\tau_1, T_m^* = T_m$
t_{Tdown}	Torque down
↓	$\tau_2, T_m^* = T_{m-down}$
t_{Tup}	Torque up
↓	Time constant G_{up}

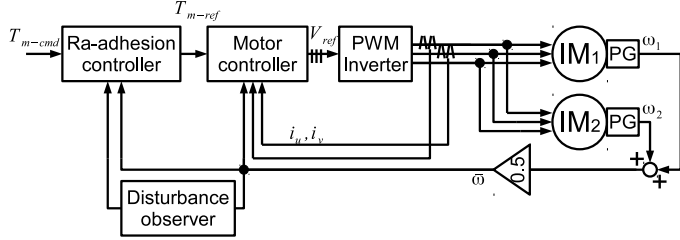


Fig. 6. Re-adhesion control based on disturbance observer and vector control (1C2M)

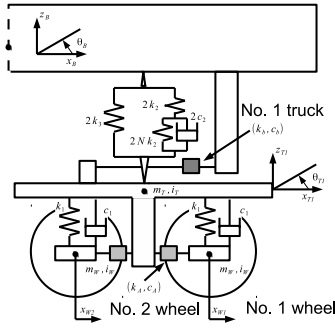


Fig. 7. 4 axle and 2 truck model (Half model)

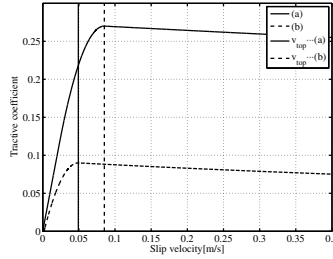


Fig. 8. Characteristic change between tractive coefficient and slip velocity ((a)... $\mu_{MAX} = 0.27$, (b)... $\mu_{MAX} = 0.09$)

III. NUMERICAL ANALYSIS MODEL

A. Numerical analysis model

We construct a rolling stock model for numerical analysis which is four axle and two truck model. In order to realize a quick torque response, we use vector control system to drive two induction motors of the truck (1C2M). This vector control system is shown in Fig. 6. Induction motor controller input uses average of two axle angular velocity and current value under assumption of the speed sensor-less vector control. The model composition is shown in Fig. 7.

B. Characteristic of the tractive force

In this paper, tractive coefficient characteristic decided by slip velocity is constructed by several parameters which are shown as follows in positive slip velocity area.

The coefficient of adhesion, μ_{MAX} is set out as the maximum coefficient of the tractive force characteristic. The micro-slip area of it is set out as a straight line whose gradient is g_1 ($g_1 > 0$). The macro-slip area of it is approximated

as exponential function which has the minimum gradient $-g_2$ ($g_2 > 0$) and converge μ_{inf} ($\mu_{inf} > 0$) at high slip velocity. The two areas are connected by parabolic function whose second order differential coefficient is $-C_{top}$ ($C_{top} > 0$). This function is given in Eq. (17). The characteristic in negative slip velocity area is formulated by its odd function property.

$$\mu(v_s) = \begin{cases} g_1 v_s & (v_s \leq v_1) \\ \mu_{MAX} - C_{top}(v_s - v_{top})^2 & (v_1 < v_s < v_2) \\ \mu_{inf} + B \exp[(v_2 - v_s) \frac{g_2}{B}] & (v_2 \leq v_s) \end{cases} \quad (17)$$

C_{top} is limited by continuity on the origin point as in Eq. (18).

$$v_1 = \frac{\mu_{MAX}}{g_1} - \frac{g_1}{4C_{top}} \geq 0, C_{top} \geq \frac{g_1^2}{4} \quad (18)$$

Assistance parameters v_1 , v_{top} , v_2 and B have been used in Eq. (17). They are defined in Eq. (19) and (20).

$$v_1 = \frac{\mu_{MAX}}{g_1} - \frac{g_1}{4C_{top}}, v_2 = \frac{\mu_{MAX}}{g_1} + \frac{g_1}{4C_{top}} + \frac{g_2}{2C_{top}} \quad (19)$$

$$v_{top} = \frac{\mu_{MAX}}{g_1} + \frac{g_1}{4C_{top}}, B = \mu_{MAX} - C_{top} \left(\frac{g_2}{2C_{top}} \right)^2 - \mu_{inf} \quad (20)$$

In the following case studies, The parameters are fixed at $g_1 = 5$, $C_{top} = 40$ and $g_2 = 0.05$ based on a measurement precedent of tractive coefficient characteristic[1].

IV. CASE STUDY SCENARIO

The case study scenario is shown in Table. IV. The simulation time span was from 0 second to 24 second. The start of the rolling stock acceleration was at 0 second from 0 km/h. When time was from 0 second to 6 second, this period had no slip. Therefore, the tractive coefficient was dropped to μ_{lim} which was less than μ_{exp} and slip started at 6 second. For example, the tractive coefficient characteristic dropped to 0.09, 0.10, 0.11 and 0.12 as shown in Fig. 9. The simulation carried out on MATLAB/simulink. Simulation step time was fixed 50 μs . Good road surface condition was shown in Fig. 8 (a).

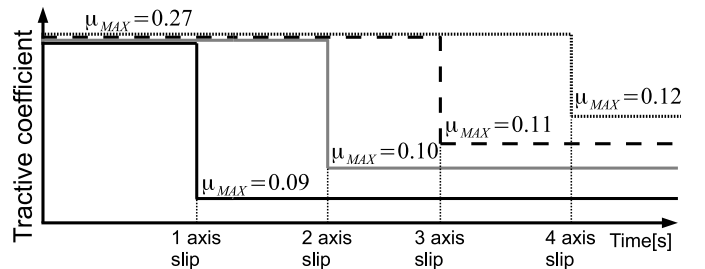


Fig. 9. Wheel condition change

Wheel condition of 1 axle was worse compared with wheel condition of 2, 3 and 4 axle shown in Fig. 9. The minimum output motor torque (T_{min}) was 10.0. The gradient was 3.0%. The parameters of a single axle bogie model were shown in Table V.

TABLE IV
CASE STUDY SCENARIO

Time [s]	Action
0	Start acceleration: $\alpha = 3.0$ [km/h/s]
	Coefficient of adhesion $\mu_{MAX} = 0.27$ Fig. 8 (a)
6	Drop coefficient of adhesion $\mu_{lim} = 0.09, 0.10, 0.11, 0.12$
15	Return coefficient of adhesion $\mu_{MAX} = 0.27$ Fig.8 (a)
24	Stop simulation

TABLE V
PARAMETERS SINGLE AXLE BOGIE MODEL

g	9.81
J	2.22×10^3
J_R	159
r	0.412
G_r	5.28

V. EVALUATION METHOD OF RE-ADHESION CONTROL

In electric railway traction, a big adhesive torque means good re-adhesion control transmitted from wheels to rail. However, in terms of the friction of rail and wheels, it is undesirable to have high adhesive torque with a slip. We suggest that a good re-adhesion control have high normalized average tractive coefficient[5] and low loss friction force around driving wheel[7] by using conflicting the evaluation method.

VI. EVALUATION OF RE-ADHESION CONTROLS BY SIMULATION

A. Motor torque and adhesive torque

In this case study, we hold the time from the slip detection time to the motor torque down time (τ_1) as 50 millisecond. We set the torque down constant (k) as 3.00. In addition, we decided the time from the slip detection time to the motor torque down time constant (G_{up}) as 1.00 second.

Motor torque and adhesive torque are shown in Fig. 10 and 11. In Fig. 10 and 11, adhesive torque is $(1 + \frac{J_R}{J})\hat{T}_L$ and motor torque is $G_r T_m$. In the adhesive condition, delta of adhesive torque ($(1 + \frac{J_R}{J})\hat{T}_L$) and motor torque ($G_r T_m$) is disturbance torque.

In Fig. 10 and 11, delta of motor torque and adhesive torque is excessive torque. Time from torque down to torque up (τ_2) was 200 millisecond. By expanding to 4 axle 2 truck model, we consider truck oscillation and axle-weight transfer, so we make latitude for re-adhesion. This proposed method successes re-adhesion control by using average information.

B. Comparison of proposed re-adhesion control and conventional re-adhesion control

1) *Conventional re-adhesion control*[6]: Conventional re-adhesion control[6] is based on static torque reduction table, to the single drive axle electric rolling stock model. At first, it was assumed that it is rare that all of two or more axes cause the idling at the same time.

Under the assumption, the detection of slip state and controller input value was deflections of velocity and acceleration on drive wheels rim. Torque reductive concept is described as follows. If deflections are near zero or less than zero,

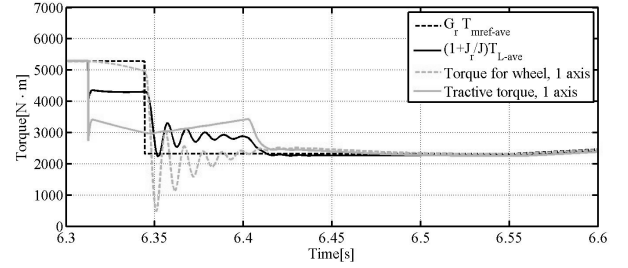


Fig. 10. Motor torque and adhesive torque (Proposed, 1 axle)

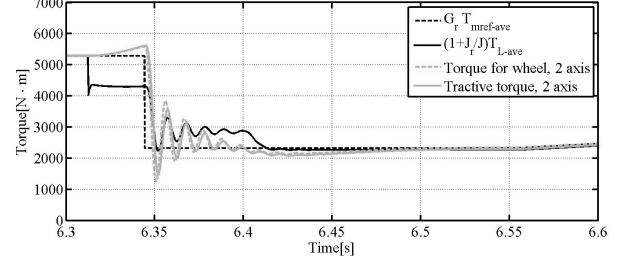


Fig. 11. Motor torque and adhesive torque (Proposed, 2 axle)

then controller assume adhesive state as micro-slip and do not reduce motor torque. Else, if one of them is big positive value, adhesive state is assumed as macro-slip state and motor torque is reduced.

Because velocity deflection can not be calculated in single drive axle model, input value of single drive axle model is only acceleration deflection. It sets subtracted driver commanded acceleration from approximate differentiated rim of wheel velocity to the rim acceleration deflection of single drive axle model.

The block diagram of re-adhesion controller is shown in Fig. 12. The non linear function has input of acceleration deflection and the output of Adl described below. If input is less than α_0 : acceleration deflection room of torque reduction, output is 1. Else if input is more than $\alpha_0 + \alpha_w$, output is 0. α_w is acceleration deflection width of torque reduction. Else if it is between α_0 and $\alpha_0 + \alpha_w$, output is applied linear supplement. Their characteristic is given in Fig. 13. The non linear function output Adl which is torque multiplicative factor to torque command from driver: T_{ref} and the multiplied value is defined as T_{adl} . Their relation is shown in Eq. (21).

$$T_{adl} = Adl \cdot T_{ref} \quad (21)$$

Therefore, value of controller output: T_{mref} is generated by LPF from T_{adl} , the re-adhesion controller has four parameters defined below.

- α_w : Acceleration deflection width of torque reduction
- α_0 : Acceleration deflection room of torque reduction
- T_u / T_d : Time constant of torque augmentation / reduction
- τ : Time constant of approximate differentiation

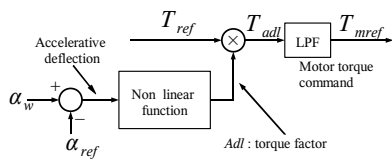


Fig. 12. A block diagram of re-adhesion controller

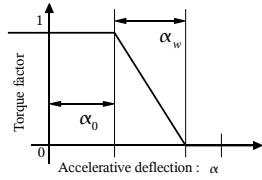


Fig. 13. Torque command reduction factor for re-adhesion control

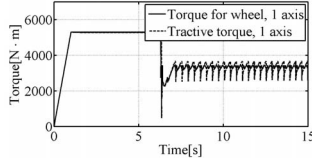


Fig. 14. Motor torque and adhesive torque (Proposed)

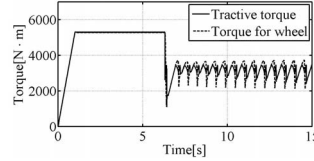


Fig. 15. Motor torque and adhesive torque (Conventional)

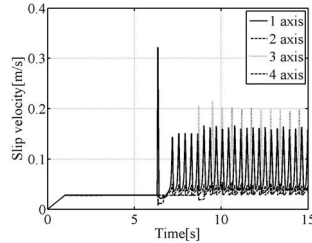


Fig. 16. Slip velocity (Proposed)

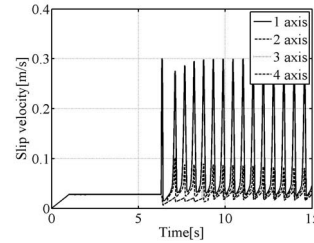


Fig. 17. Slip velocity (Conventional)

2) Comparison of normalized average tractive coefficient and loss friction force around driving wheel: In this section, we compared the proposed re-adhesion control with the conventional re-adhesion control[6]. Motor torque and adhesive torque of each methods is shown in Fig. 14 and 15. Slip velocity of each method is shown in Fig. 16 and 17. The adhesion characteristic and loss friction force around driving wheel are shown in Table VI. The proposed re-adhesion control (1C1M) has much information such as each motor torque and angular velocity, so normalized average tractive coefficient is the best value of three method. Table VI shows that the adhesion characteristic of the proposal method was 7.04 % better than the conventional method. In addition, the loss friction force around driving wheel did not change. These improvements depend on two points.

- 1) To shorten the time to slip detection, the proposed re-adhesion control reduces the excessive angular momentum.
- 2) To achieve high adhesion characteristic without slip by the small torque down constant k and the torque up time constant (G_{up}).

VII. CONCLUSION

This paper proposed a new slip re-adhesion control based on the excessive torque and excessive angular momentum. The effectiveness of the proposed method has been confirmed

TABLE VI
COMPARISON BETWEEN CONVENTIONAL AND PROPOSAL RE-ADHESION CONTROL

Method	Normalized average tractive coefficient $\bar{\mu}_{ur}$	Loss friction force around driving wheel F_{slip}
Proposed (1C2M)	85.2% (100%)	54.5 (100%)
Proposed (1C1M)	89.1% (4.58% ↑↑)	89.7 (64.6% ↑↑)
Conventional[6] (1C2M)	79.6% (7.04% ↓↓)	53.7 (1.47% ↓↓)

by the mathematical analysis under poor track condition with $\mu_{MAX} = 0.09$. Furthermore, the proposed method has been evaluated by two performance indicators. In this case study, the merits of the proposed re-adhesion have been shown as follows.

- 1) The proposed re-adhesion control can accurately re-adhere by a set time slip.
- 2) It can find when rail and wheels re-adhere by making reparation for the excessive angular momentum.
- 3) It does not need to do the sequential calculation by the simple calculation such as the rectangle and triangle of the excessive torque (T_{ex}).

We did parameter analysis of the proposed re-adhesion control by using these two evaluation method. As a result, adhesion characteristic of the proposed method was 7.04 % better than the conventional method. In addition, the loss friction force around driving wheel did not change.

In the future, this case study use 1C2M model (1 inverter 2 motor drive system), so it is considered to extend 1C4M model (1 inverter 4 motor drive system). In addition, the proposed re-adhesion control need to be confirmed in real train test.

REFERENCES

- [1] K. Nagase : The realities of adhesion between rail wheels on main line (result of the survey by slipping adhesive bogie),
- [2] Technical committee of adhesion control technology investigation in railway system: Adhesion control technology in railway vehicle, IEEJ technical report No.673 (in Japanese) , 1998 , pp. 28-34
- [3] O. Kiyoshi, O. Yasuaki, N. Ken, M. Ichiro, Y. Shinobu : An Approach of Anti-slip Re-adhesion Control of Electric Motor Coach Based on First Order Disturbance Observer, Trans. Inst. Electr. Eng. Jpn., vol. D, 120, 3, pp.382.389 (2000-3)
- [4] S. Kadowaki, K. Oishi, I. Miyashita, S. Yasukawa : Anti-Slip Re-adhesion Control of Electric Motor Coach(2M1C) Based on Disturbance Observer and Speed Sensor-less Vector Control, Trans. Inst. Electr. Eng. Jpn., vol. D, 121,11,pp.1192.1198 (2001-11)
- [5] S. Kadowaki, T. Hata, H. Hirose, K. Oishi, N. Iida, M.Takagi, T. Sano, S. Yasukawa : Application Results and Evaluation of Anti-slip Re-adhesion Control Based on Speed Sensor-less Vector Control and Disturbance Observer for Electric Multiple Units, Series 205-5000, Trans. Inst. Electr. Eng. Jpn., vol. D, 124, 9, pp.909.916 (2004-9) Proc. Japan Society of Mechanical Engineers the paper collection, (in Japanese), Vol.504-C, (1988 Aug)
- [6] H. Iida, S. Kita, M. Kumano, and T. Kikuchi : Development of Fuzzy Adhesive Control System, Proc. the 1995 National convention record I.E.E.Japan Industry Applications Society. , (in Japanese), Vol.2 pp. 269-272 (1995)
- [7] T. Hara, Y. Tsukinokizawa, T. Koseki : Study on Re-adhesion control by monitoring excessive angular momentum in electric railway traction, 2011 Annual Conference of IEEJ. Industry Applications Society, Okinawa, Sep 6th -8th 2011.